1   **Study on Properties of New Biodegradable Plant Fiber (Agave Decipiens) for Polymer**

2   **Reinforcement**

3

4   Aravinth K[1*], Ramakrishnan T[2]

5   [1]Research Scholar, Department of Mechanical Engineering, Sri Eshwar College of Engineering,

6   Coimbatore, Tamil Nadu-641202, India.

7   [2]Associate Professor, Department of Mechanical Engineering, Sri Eshwar College of Engineering,

8   Coimbatore, Tamil Nadu-641202, India.

9   [*]Corresponding author:

10   E-mail: *aravinth.k2021ftscholar@sece.ac.in*, tel: +91 - 9025614583

11 **GRAPHICAL ABSTRACT**

12

13

14

15

16

17

18

19

20

21

22

23

24

25

26

ABSTRACT

The article involves in the process of study on novel plant fiber from agave plant species known as agave decipiens. The fiber was mechanically extracted from their leaves and fiber was chemically treated using sodium hydroxide by 5% (w/v). Using various analyses, the fiber was characterized and its properties were obtained. From chemical constituent analysis it was confirmed that hemicellulose, amorphous lignin, and other impurities were removed to some extent, and using x-ray diffraction (XRD), an improvement in crystallinity index (CrI) was observed (i.e. from 47.99% to 52.29%). Increased crystallinity provides better tensile stress from 479.302 MPa to 494.172 MPa, which was confirmed by single fiber tensile test. A change in physical diameter was observed using a digital microscope, the outer diameter was reduced to 117.66μm from 121.84μm. Change in chemical components was identified by Fourier Transform Infrared Spectroscopy (FTIR). Alkaline-treated (AT) fiber sustains a temperature of about 240°C during thermogravimetric analysis (TGA). Study on surface morphology was conducted with help of scanning electron microscope (SEM). Concluding that alkaline treatment made some impact on fiber characteristics and made it suitable for reinforcement.

Keywords: Biomaterial, Natural Fiber, Agave Decipiens, Alkaline Treatment, Cellulose, Crystallinity

1. Introduction

Materials having excellent mechanical property and less impact on the environment has prompted a slew of studies into bio-sourced polymer composites. Plant-based fibers attract the most scientific interest of any natural fiber because they are abundant, cost-effective, bio-degradable, and they possess reasonable mechanical strength (Santos et al., 2022). Characteristics of natural fibers are primarily influenced depending on fiber constituents like hemicellulose, amorphous lignin, cellulose, and other impurities say wax and dust particles. Fiber strength and stiffness were determined by the presence of these chemical components (Krika et al., 2021; Ramakrishnan et al., 2022).

Mostly all plant fibers were made-up of intricate structure, which contains a center channel as a lumen and covered by the cell wall. Lumen layer is used to transport food and water. The cell wall is made up of 3 layers: primary wall, secondary wall, and middle lamella. Primary wall consists of lignin, cellulose, pectin, and hemicelluloses. Crystalline cellulose will present in the secondary wall and it was surrounded by other chemical constituents. Hemicelluloses are adhered around the cellulose using hydrogen bonding, while the intermediate wall/lamella offers structural properties to the fiber. In plant fiber percentage of micro-fibril angle, cellulose, and hemicelluloses rules the strength of the natural fibers, which also differs from plant to plant (Latif et al., 2019). The fiber strength can be improved by various surface modifications, and an altered fiber surface has less attractive to moisture. That is hydroxyl group gets eliminated from the fiber which lowers the hydrophilic property (Kabir et al., 2012).

Komal et al., (2018) took 5% (m/v) sodium hydroxide solution for treating the banana fiber about 5 hours. The author confessed that fiber resin interfacial bonding and thermal stability were improved after chemical modification. Fractography justifies the change in the percentage of chemical components in untreated (UT) fiber and alkaline-treated (AT) fiber. Guo et al., (2019) modified kenaf fiber using 5% sodium hydroxide followed by other oxidizing agents. The reduction of chemical constituents in the fiber was evident by chemical composition analysis, TGA, and FTIR tests. The author noticed that after chemical treatment, the fiber had less moisture absorption and improved

4

crystalline index and tensile strength. The author confirmed that solely alkaline treatment itself removes most of the chemical constituents from the fiber, if much improvement is required alkaline followed by hydrogen peroxide treatment was suggested. Hamidon et al., (2019) concludes that surface modification increases the bonding between fiber and resin. Such treatment also reduces water adsorption i.e. hydrophilic property gets diminished. Mostly all surface treatments aided to improve fiber properties, fiber suitability, and fiber-resin adhesion. Mentioned that chemical treatment up to certain concentrations increased the mechanical properties and also provides better bonding between fiber and resin. Over the optimum concentration, alkaline treatment reduces mechanical characteristics. Water absorption also gets reduced because of the chemical treatment. Changes in fiber characteristics are observed using SEM and FTIR analysis and thermal behavior using TGA/DTG analyses (Venkatachalam et al., 2016).

Neto et al., (2019) carried out alkaline and saline treatment for hybrid fibers (jute, sisal, ramie, curaua). Used 2g of NaOH in 100ml of water and soaked the fibers for one hour and followed by a saline solution maintained under a pH of 5. The author admits that alkaline treatment increases fiber roughness and chemical treatment improves the fiber's thermal stability. Sgriccia et al., (2008) experimented with kenaf, flax, and hemp fibers by treating them using 5% sodium hydroxide solution for about an hour and followed by saline treatment. Author noted that lignin and hemicellulose are removed from the fiber, and traces of saline coating was observed using SEM. Thespesia Lampas plant fiber was immersed in a 2% (w/v) alkaline solution and left for one day. The finding revealed that mechanical strength of alkaline-treated (AT) fiber was better than untreated (UT) fiber. Fiber roughness was examined using SEM micrographs. Other analyses like chemical analysis, FTIR, XRD, and TGA support the chemical treatment done (Reddy et al., 2014). Prithiviraj and Muralikannan, (2022) performed a surface modification using 5% NaOH alkaline solution for perotis indica fiber under different soaking times say, 1min, 30mins, 45mins, 60mins, and 75mins. The author concluded that fiber tensile value was improved in 60mins of soaking time compared to other timings. From TGA and DTG curves, thermal property of the fiber increased to 20°C. XRD analysis

proves that the crystalline index got raised from 48.3% to 55.43%. Presence of cellulosic components was proved by the FTIR spectrogram. The survey indicates that alkaline treatment can affect the surface of the fiber by eliminating undesirable substances, leading to a higher percentage of cellulose. This ultimately increases the fiber's strength, making it a viable material for polymer reinforcement. So, it is an indeed requirement to alter the fiber properties through chemical treatment mostly by alkaline solution.

Natural fiber-reinforced composite opens up new opportunities for all scientists and researchers, with an emphasis on the advantages of generating bio-degradable materials. From decades to the current scenario, enormous novel plant fiber varieties like abutilon indicum, saccharum bengalense grass, vernonia elaeagnifolia, purple bauhinia, furcraea foetida, juncus effusus L., cryptostegia grandiflora, fibers from stems of leucasaspera, cardio spermum halicababum, derris scandens, grewia damine, cissus vitiginea, barks of vachellia farnesiana, areca palm leaf stalk, calotropis gigantea fruit bunch, fiber from ficus religiosa tree roots, etc., were identified, characterized, and providing an alternative resource for composite reinforcement instead of synthetic fibers.

The study introduces a novel fiber (agave decipiens plant fiber) to the list of discovered novel fibers. The properties of agave decipiens fiber were not discovered or studied by any researchers and no significant research had examined predominantly in field of natural fiber composites. The study involves in the process of investigating the vital properties of untreated (UT) and alkaline-treated (AT) agave decipiens fiber to find its reinforcing capability in polymer composites

2. Resources and Techniques

2.1. Extraction of Fiber

Large, mature, fresh agave decipiens leaves were identified and obtained from the rural areas of Coimbatore district, Tamil Nadu, which was shown in figure 1. At first, agave decipiens leaves were cut down from the plant, then the thrones at the two edges of the leaves were removed using a normal knife. Fibers were extracted using mechanical decortication method. By feeding the leaves inside a fast-rotating cylindrical roller, the pulps from the leave were removed by leaving the fiber alone.

122   Next, the fiber was washed 2-3 times to remove the contaminates and it was allowed to dry in open

123   sunlight. Figure 2, shows the extraction of agave decipiens fiber (Kathirselvam et al., 2019; Kumar

124   and Sekaran, 2014; Thirumalaisamy and Subramani, 2018).
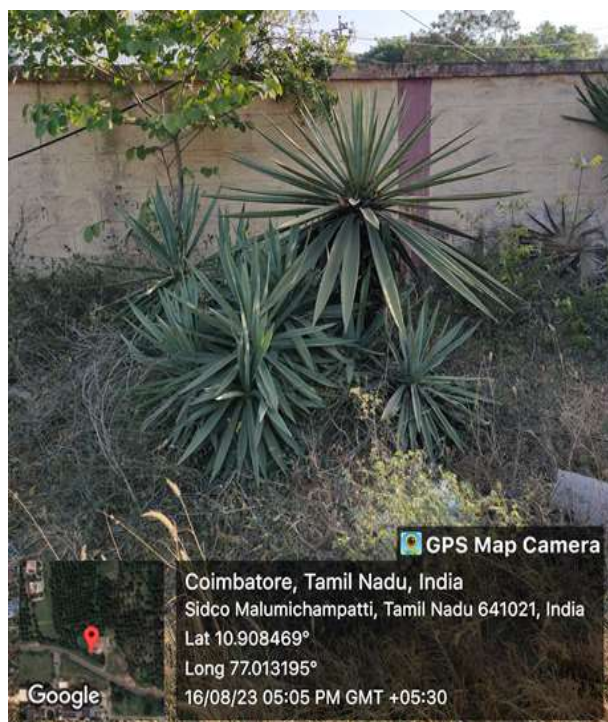
125

126   **Figure 1.** Agave Decipiens plant

127

128   **Figure 2.** Extraction of fiber from leaves

129   *2.2. Surface Treatment*

130   The extracted raw fiber contains impurities and unwanted chemical substances over the fiber surface.

131   So it cannot be directly used for reinforcement. If raw fiber was utilized for reinforcement without

132   chemical processing there occurs a poor interlocking between fiber and resin, which obviously

                                                                                                        7

133 decreases the laminate strength. Water absorbance will easily take place because of the presence of

134 hydroxyl functional group (–OH) in the form of hemicellulose. Considering these negative impacts,

135 it is preferred to perform a chemical treatment. There are various types of fiber chemical treatment

136 available and from which alkali treatment provides better results (Hamidon et al., 2019; Ramshankar

137 et al., 2023; Venkatachalam et al., 2016).

138 For this research work, based on the literature study alkaline (NaOH) chemical treatment was

139 performed for the new cellulosic agave decipiens plant fiber. At first, the fiber was cleaned with fresh

140 water and immersed in a sodium hydroxide solution prepared with 5% (w/v) concentration and

141 allowed to soak for up to 3 hours. Figure 3 demonstrates the alkaline treatment for agave decipiens

142 fiber. The fiber was then rinsed once again with fresh water to eliminate any remaining sodium

143 hydroxide traces, and dried at 100°C for half an hour. (Guo et al., 2019; Komal et al., 2018; Prithiviraj

144 and Muralikannan, 2022; Sgriccia et al., 2008).

146 **Figure 3.** Alkali (NaOH) Treatment 5% (w/v)

147 *2.3. Experimental Analysis*

148 *2.3.1. Diameter Measurement*

149 Fiber diameter measurement is an essential function by which change in the diameter after alkaline

150 treatment can be observed and it was very useful in calculating the fiber tensile value based on

151 equation 1 (Guo et al., 2019; Puspita et al., 2023). A digital microscope was used for diameter

152 measurement. Measurement was taken at various points and the average value can be calculated. To

153   do this 25 samples of fibers each from both untreated (UT) and alkaline-treated (AT) fibers were

154   used.

155   *2.3.2. Single Fiber Tensile Test*

156   As per ASTM D3822-07 (Ding et al., 2022; Moshi et al., 2020), tensile strength of agave decipiens

157   fiber (ADF) was tested using Zwick Roell Z010 tensile tester. 25 numbers of single fiber were

158   randomly taken in both UT and AT fibers. Maintained a gauge length of around 75mm by constantly

159   moving the crosshead at 5mm/min. The tensile test results provide the maximum load at which the

160   fiber fails with respect to % of elongation.

161     $$\text{Tensile stress} = \frac{\text{Maximum Load at Failure}}{\text{Area of the fiber}}$$

162     $$\text{Tensile stress} = \frac{F_{max}}{\frac{1}{4}\pi d^2} \qquad\qquad (1)$$

163   Where F_{max} is the maximum force at fiber failure and d denotes the diameter or cross-section

164   (considering fiber has a circular cross-section)

165   *2.3.3. X-Ray Diffraction analysis*

166   Fiber crystallinity was evaluated by Rigaku Ultima IV X-Ray diffractometer having Cu as target

167   element used for the XRD measurement. The radiation was measured at 2θ between 5° and 60° under

168   the rate of 2°/min with 0.001° step size. Equation 2 is known as Segal empirical method (Ding et al.,

169   2022; Prithiviraj and Muralikannan, 2022; Vijay et al., 2020) which was used to calculate the CrI

170   based on the peak intensities observed in the XRD chart. Using Debye–Scherrer equation 3 (Babu et

171   al., 2022; Liu et al., 2019; Madhu et al., 2019) the crystalline size (CrS) of the fiber was calculated.

172     $$\text{\% of CrI} = \left(\frac{I_{200} - I_{100}}{I_{200}}\right) X\ 100 \qquad\qquad (2)$$

173   Where, I_{200} – Amorphous Peak Intensity, I_{100} – Crystalline Peak Intensity

174     $$\text{CrS} = \frac{k\,\lambda}{\beta\,\cos\theta} \qquad\qquad (3)$$

175   Where, I_{200} – Amorphous Peak Intensity, I_{100} – Crystalline Peak Intensity. In equation (3), the
176   Scherrer constant (0.89) is provided for k, λ known as X-ray radiation's wavelength (0.154 nm), β is

177 referred to as full width at half maximum (FWHM) diffraction peak obtained from XRD peak, Bragg
178 angle was denoted by θ.

179 *2.3.4. Physico-Chemical Analysis*

180 Chemical composition analysis of fiber is important to predict the presence of various chemical
181 components, which gives the percentage of constituents that have been removed through alkali
182 treatment. Based on the survey, pycnometer was used to measure the fiber density, where liquid
183 toluene a known density (0.866 g/cc) was used as an immersion liquid (Kathirselvam et al., 2019;
184 Ravindran et al., 2020). Cellulose was identified by Kursher and Hoffer's method and Conrad method
185 was performed to identify the wax content (Manimaran et al., 2018; Khan et al., 2021; Rajeshkumar
186 et al., 2021; Udhayakumar et al., 2023; Vijay et al., 2022). Hemicellulose and lignin were predicted
187 using NFT 12-008 (Ganapathy et al., 2019; Rajeshkumar et al., 2021; Vijay et al., 2022) and Klason
188 method respectively (Shanmugasundaram et al., 2018; Vijay et al., 2021). Finally, Sartorius MA45
189 moisture analyzer was used to find the moisture content and ash content known by ASTM E1755-01
190 (Khan et al., 2021; Moshi et al., 2020; Vinod et al., 2021).

191 *2.3.5. Fourier Transform Infrared Spectroscopy*

192 Chemical components in the form of chemical/functional bonds were observed using Schimazu IR
193 Affinity 1S FTIR spectroscopy. With the help of functional group identification, change in the
194 chemical components before and after alkaline treatment was identified using FTIR spectroscopy. To
195 do this 2mg of fiber was crushed and mixed with zinc selenide (ZnSe) crystal for spectrum absorbance
196 in a pallet shape and size. The spectral wavelength was measured between $4000cm^{-1}$ to $400cm^{-1}$ with
197 a resolution of $0.5cm^{-1}$.

198 *2.3.6. Thermogravimetric Analysis*

199 SDT Q600 analyzer (TA Instruments) was used to investigate the thermal stability of agave decipiens
200 fiber. A platinum crucible containing 2.5mg of powdered fiber was used for TG analysis, experiment
201 was conducted between the temperature of 25°C and 700°C maintaining a constant heating rate of
202 10°C/min under the influence of nitrogen environment. Due to change in the temperature, constituents
203 present in the fiber gets decomposed, which results in weight reduction.

204 *2.3.7. Differential Scanning Calorimetry*

205 DSC Q20 (TA Instruments) was utilized to investigate the different thermal transition phases in

206 untreated (UT) and alkaline treated (AT) agave decipiens fiber. To perform this analysis, fiber

207 measuring of 2mg was taken in an aluminum pan and a heating rate of 10°C/min was maintained. The

208 complete heat flow study was done under a nitrogen gas atmosphere within the temperature range of

209 20°C to 400°C.

210 *2.3.8. Scanning Electron Microscope*

211 Outer structure, presence of porosity, and fiber surface roughness were observed using scanning

212 electron microscope (SEM). Micrographs of UT and AT fiber were obtained using ZESSIS FESEM

213 SIGMA VP 03-04 scanned at 2 kV. Meanwhile, natural fiber is a non-conductive material before

214 conducting SEM analysis sputtering coating was performed to get clear views of micrographs.

215 **3. Results and Discussion**

216 *3.1. Diameter measurement*

217 Sample measurement of fiber diameter using a digital microscope was given in figure 4. Alkali

218 treatment will have an impact on the fiber diameter. After alkaline treatment, fiber diameter gets

219 reduced due to the elimination of unwanted impurities, cellulosic components, and waxy substances

220 present over the fiber's outer surface (Chakravarthy et al., 2020; Guo et al., 2019; Maache et al., 2017;

221 Moshi et al., 2020; Udhayakumar et al., 2023). Diameter values of UT and AT of the agave decipiens

222 fiber were given in table 1.

223

224 **Figure 4.** Sample diameter measurement of agave decipiens fiber (ADF)

225 *3.2. Single Fiber Tensile Test*

226 As mentioned in the methods session, output of tensile test for a single fiber was obtained in the form

227 of maximum load at fiber failure with respect to % of elongation. From the experimental values of

228 UT and AT fiber, the average maximum force and percentage of elongation at break were statistically

229 calculated and tabulated in table 1.

230 **Table 1.** Diameter values and experimental results of single fiber tensile test

Fiber Type	Diameter (μm)	The maximum force (F_{max}) (N)	% of elongation
UT fiber	121.84	5.5 N	2.8
AT fiber	117.66	5.3 N	2.3

231 Fiber tensile strength can be calculated using equation 1 and using hook's law, the elastic modulus of

232 the fiber can be calculated, which was given in table 2.

233 **Table 2.** Mechanical property of the UT and AT fiber

Fiber Type	Strain	Tensile Strength (MPa)	Elastic modulus (GPa)
UT fiber	1.028	479.302	0.466
AT fiber	1.023	494.172	0.483

234 From table 2, it can be clearly understood that untreated fiber possesses less tensile value and less

235 elastic modulus compared to alkaline-treated fiber. By the removal of unwanted substrates after

236 chemical treatment, new hydrogen bonds are created with cellulose elements which results in the tight

237 packing of elements between the interfibrillar region. Thus making the fiber more resistant to the load

238 applied (Maache et al., 2017; Reddy et al., 2014; Udhayakumar et al., 2023).

239 *3.3. X-Ray Diffraction analysis*

240 Using diffractogram, it was observed that there are two peak curves one is at minimum called

241 amorphous peak (I_{100}) which contains cellulose, hemicellulose, amorphous lignin, and other

242 impurities, and another peak at a maximum value called crystalline peak (I_{200}) which contains α-

243 cellulose (Ding et al., 2022; Prithiviraj and Muralikannan, 2022; Vijay et al., 2020). Figure 5 provides

244 the diffractogram of UT and AT fiber. From the analysis, it was noted that I_{100} (Intensities) for UT

245 and AT fiber was 5591.67 ($2\theta=16.12^{\circ}$) and 10473.3 ($2\theta=16.06^{\circ}$) respectively, then I_{200} (Intensities)

246 for UT and AT fiber was 10751.7 ($2\theta=22.16^{\circ}$) and 21,955 ($2\theta=22.24^{\circ}$) respectively. Calculated values

247 of CrI and CrS were tabulated in table 3.

248 **Table 3.** Calculated values of CrI and CrS for UT and AT fiber

Type of Fiber	Crystallinity Index	Crystalline Size (nm)
Untreated Fiber	47.99%	2.980
Treated Fiber	52.29%	4.721

249 Using equation 1, The crystallinity index of UT and AT of agave decipiens fiber (ADF) was

250 determined to be 47.99% and 52.29%, respectively. From the graph, it can be noted that untreated

251 ADF has a lesser intensity peak compared to alkaline-treated ADF, which proves that after alkali

252 treatment mostly all amorphous constituents were removed and the crystallinity of fiber gets

253 improved due to the increase in cellulose percentage. An increase in CrI is directly proportional to

254 the increase in fiber mechanical properties and this could be the cause for the increase in tensile value

255 of the AT fiber. Higher CrI indicates the reduction in moisture due to the absence of -OH molecules,

256 which was proved by the crystalline size (CrS). Untreated fiber has 2.980nm and alkaline-treated

257 fiber has 4.721nm of CrS. The crystalline size was increased after alkali treatment which signifies

258 that the hydrophilic property gets reduced (Babu et al., 2022; Liu et al., 2019; Madhu et al., 2019).
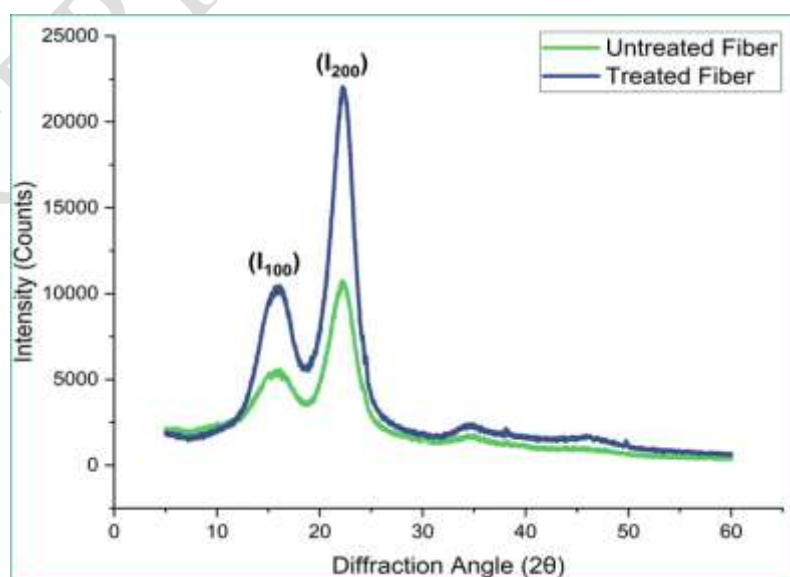
259

260 **Figure 5.** Diffractogram of UT and AT of agave decipiens fiber

13

3.4. Physico-Chemical Composition Analysis

Every plant fiber consists of cellulosic (cellulose, hemicellulose, and lignin) and non-cellulosic (wax and impurities) substances. Depending on the type of plant, the climate, the soil in which the plant is grown, etc., the distribution of these components will change. Based on these components fiber properties like mechanical strength and thermal stability were determined (Jaiswal et al., 2022; Vijay et al., 2022). Table 4 gives the percentage distribution of chemical components in agave decipiens fiber.

After alkaline treatment, it can be seen that the decrease in hemicellulose was from 27.82% to 23.67%. Since hemicellulose readily reacts with NaOH (alkaline treatment) and gets detached from the fiber. Lignin has less sensitive to the action of sodium hydroxide so the removal of lignin was less which is about from 12.36% to 10.23%. The elimination of hemicellulose and some percentage of lignin after alkaline treatment decreases moisture absorption property of the fiber that is from 15.73% to 10.58%, in other words, hydrophilic characteristics get diminished, and fiber is now well suited for reinforcement with a matrix. Due to the elimination of contaminates after alkali treatment, the overall percentage of cellulose gets increased which is from 61.79% to 69.10%. An increase in cellulose percentage will significantly improve the fiber crystalline property that directly increases the fiber's mechanical strength.

Raw agave decipiens have higher cellulose content compared to other novel fibers like saccharum bengalense grass, Ficus religiosa, Grewia damine, phoenix pusilla, and thespesia lampus. Phaseolus vulgaris, Derris scandens, Calpotropis gigantean fruit, Cissus vitiginea, and perotic indica have higher cellulose than raw agave decipiens fiber. Table 5 compares the density and presence of various chemical components of agave decipiens with other natural fibers.

During reinforcement, wax content may lead to poor bonding between fiber and resin, that lower the mechanical property as well as the tribological property of the composite. After alkaline treatment, wax content was reduced to 0.25%. The percentage of components present in the fiber was likely removed after chemical treatment, as evidenced by the decrease in ash content from 3.71% to 3.22%.

Table 4. Various chemical constitutions of UT and AT fiber

Chemical constitutions	UT Fiber	AT Fiber
Cellulose %	61.79	69.10
Hemicellulose %	27.82	23.67
Lignin %	12.36	10.23
Wax %	0.48	0.25
Ash %	3.71	3.22
Moisture %	15.73	10.58
Density (g/cc)	0.89	1.17

Finally, fiber density was increased from 0.890 (g/cc) to 1.17 (g/cc) after chemical modification. This is because of the removal of non-cellulosic particles having smaller density values and the filling of chemical molecules in between the voids and pores on the fiber surface. Agave decipiens fiber has lesser density, so it can be employed in lightweight applications. All of the preceding statements disclose that the alkaline treatment has an influence on the agave decipiens fiber and that it is appropriate for reinforcing in polymer composites.

Table 5. Comparison of density and various chemical compositions of agave decipiens fiber with other fibers from different sources

Different natural fiber		Cellulose %	Hemicellulose %	Lignin %	Wax %	Moisture %	Density (g/cc)	Reference
Agave Decipiens	UT Fiber	61.79	27.82	12.36	0.48	15.73	0.890	Current work
	AT Fiber	69.10	23.67	10.23	0.25	10.58	1.170	
Saccharum bengalense grass		53.45	31.45	11.7	1.3	2.1	1.165	Vijay et al., 2020
Ficus religiosa		55.58	13.86	10.13	0.72	9.33	1.246	Moshi et al., 2020
Grewia damine		57.78	14.96	16.65	0.59	-	1.378	Ravindran et al., 2020
Phoenix pusilla		59.46	18.56	8.28	0.33	-	0.211	Madhu et al., 2019
Thespesia lampus		60.63	26.64	12.70	0.76	10.83	1.412	Reddy et al., 2014

Phaseolus vulgaris	62.17	7.04	9.13	0.36	6.1	0.934	Babu et al., 2022
Derris scandens	63.3	11.6	15.3	0.81	6.02	1.430	Sarala et al., 2020
Calpotropis gigantean fruit	64.47	9.64	13.56	1.93	7.27	0.457	Narayanasamy et al., 2020
Cissus vitiginea	65.43	14.61	10.43	0.39	8.47	1.287	Chakravarthy et al., 2020
Perotic indica	68.4	15.7	8.35	0.32	9.54	-	Prithiviraj and Muralikannan, 2022

3.5. Fourier Transform Infrared Spectroscopy

FTIR was analyzed for both UT and AT fiber which was given in figure 6 and various absorbance peaks with respective functional groups was tabulated in table 6. The wave absorbance between $3800cm^{-1}$ and $3000cm^{-1}$ shows the existence of (-OH) hydroxyl functional group, which indicates that moisture content was available in both AT and UT fiber (Madhu et al., 2019; Madhu et al., 2020; Manimaran et al., 2018; Narayanasamy et al., 2020; Ravindran et al., 2020). Two peak absorbances say $2924.08cm^{-1}$ and $2860.43cm^{-1}$ were noticed between the wave band $3000cm^{-1}$ and $2500cm^{-1}$. This peak occurrence happened by stretching of methyl functional groups that are (CH-) and (CH_2-). In alkaline-treated fiber, less absorbance was noticed in the respective two peaks because of the elimination of hemicellulose after alkaline treatment (Babu et al., 2022; Liu et al., 2019; Madhu et al., 2019; Narayanasamy et al., 2020; Sarala et al., 2020). Stretching vibration of alkyne functional group ($C{\equiv}C$) can be absorbed in the peak wavenumber $2158.35cm^{-1}$, which relates to the wax substance present in the fiber (Madhu et al., 2019; Madhu et al., 2020; Moshi et al., 2020; Sarala et al., 2020).

Peak absorbance between $1750cm^{-1}$ and $1500cm^{-1}$, $1730.14cm^{-1}$ peak was exhibited in UT fiber which shows the stretching of carboxyl and ester functional groups (–COO), indicating the existence of hemicellulose and lignin. Meanwhile, this peak absorbance was zero in AT fiber because of the elimination of hemicellulose and some amount of lignin (Ding et al., 2022; Liu et al., 2019; Shaker et al., 2020; Vijay et al., 2020). The peak absorbance noticed at $1653cm^{-1}$ and $1656.85cm^{-1}$ in the UT

16

fiber and AT fiber respectively signifies the vibration of carbonyl and acetyl functional groups (C=O), from this presence of some percentage of hemicellulose and lignin, can be confirmed (Babu et al., 2022; Moshi et al., 2020; Ravindran et al., 2020;). Stretching of alkene functional group (C=C) occurs at the wavelength of $1529.55 cm^{-1}$ and $1517.97 cm^{-1}$ in the AT and UT fiber respectively, which indicates the presence of aromatic lignin (Ding et al., 2022; Vijay et al., 2020).

Three peaks absorbance say, $1402.25 cm^{-1}$, $1317.38 cm^{-1}$, and $1261.45 cm^{-1}$ were noticed between the wavelength $1500 cm^{-1}$ to $1250 cm^{-1}$, which attributes to methyl and acetyl functional groups. This indicates the existence of cellulose (CH_2-) and aromatic lignin, hemicellulose (C-O) respectively (Sgriccia et al., 2008; Shaker et al., 2020). Peak absorbance at $1317.38 cm^{-1}$ was present only in alkaline-treated fiber indicating the increase in cellulose percentage after alkali treatment. Wavelength absorbance between $1250 cm^{-1}$ and $1000 cm^{-1}$, a sharp narrow peak absorbance can be seen in untreated fiber at $1122.57 cm^{-1}$ and $1022.27 cm^{-1}$, which attributes to the bending of (C-O-C) and (C-O) which indicates the existence of polysaccharides of cellulose and pyranose ring of cellulose respectively. A board peak absorbance was noticed at $1138 cm^{-1}$ wavelength because of the improvement in cellulose percentage in AT fiber (Guo et al., 2019; Moshi et al., 2020). The β-glucosidic linkage between the monosaccharide of cellulose occurs at the peak wavelength of $806.25 cm^{-1}$ and $887.26 cm^{-1}$ (Chakravarthy et al., 2020; Liu et al., 2019; Reddy et al., 2014; Maache et al., 2017). Final peak can be witnessed at $607.58 cm^{-1}$ which was accredited to (C-OH) and occurs due to out-of-plane bending of cellulose (Ding et al., 2022; Guo et al., 2019; Sarala et al., 2020). FTIR analysis confirmed the presence of chemical components in the fiber with the aid of functional groups It was also possible to determine how the chemical composition changed in proportion followed by alkaline treatment. FTIR inference proves that cellulose percentage was increased due to chemical treatment.

Table 6. Wavenumber and presence of functional groups identified using FTIR analysis

Wavenumber (cm^{-1})	Absorbance		Chemical composition	Functional groups
	UT Fiber	AT Fiber		

17

| 3800 - 3000	All peaks within the range		(-OH)	Hydroxyl groups
3000 - 2500	2924.08, 2860.43		(CH-) & (CH$_2$-)	Methyl groups
2500 - 1750	2158.35		C≡C	alkynes
1750 -1500	1730.14	-	(–COO)	carboxyl and ester
	1653	1656.85	(C=O)	carbonyl and acetyl
	1517.97	1529.55	(C=C)	alkene
1500 - 1250	1402.25		(CH$_2$-) & (C-O)	methyl and acetyl
	-	1317.38		
	1261.45			
1250 - 1000	1122.57	1138	(C-O-C) & (C-O)	polysaccharides of cellulose and pyranose ring of cellulose
	1022.27			
1000 - 750	887.26, 806.25		-	β-glucosidic linkage of cellulose
750 - 500	607.58		(C-OH)	Out-of-plane bending of cellulose
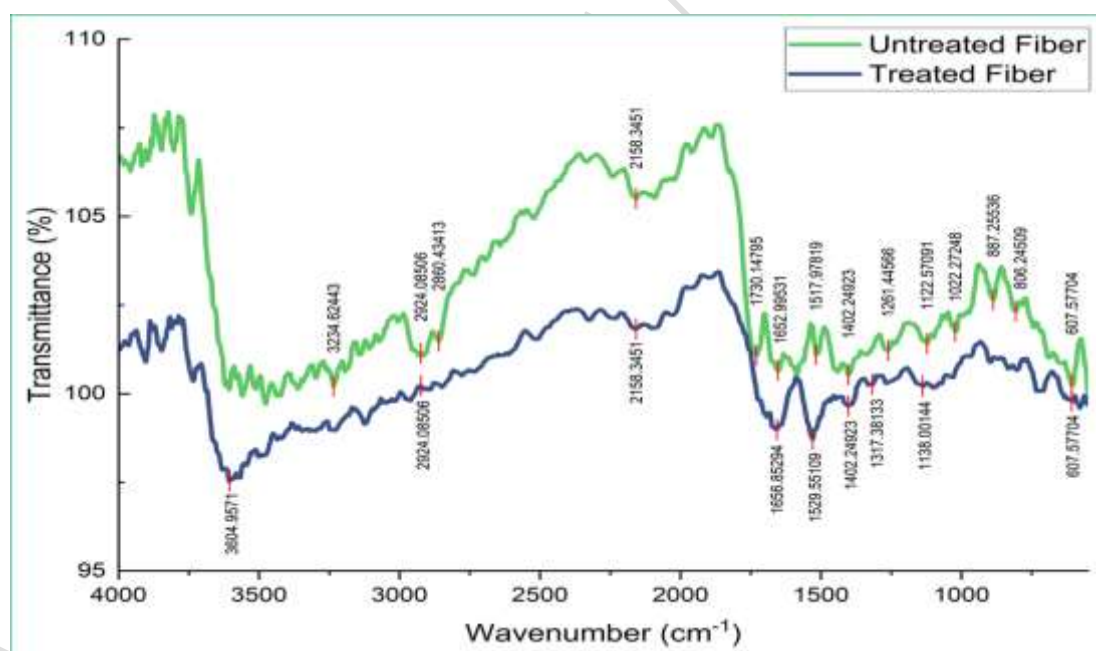
Figure 6. FTIR spectroscopy for UT and AT fiber

3.6. Thermogravimetric Analysis

Decomposition of elements and fiber's thermal stability can be studied using thermogravimetric analysis. Figure 7 and figure 8 gives the detailed interpretation of TGA and DTG curves for UT and AT agave decipiens fiber and summarized values of TGA results were tabulated in table 7. Thermal

18

345 stability can be identified by the percentage of weight loss at an increasing order temperature

346 (Narayanasamy et al., 2020; Shaker et al., 2020).

347 The curve can be divided into 4 regions. In the first region viz., presence of moisture in the fiber

348 absorbs the temperature and evaporates which results in slight weight reduction, which can be seen

349 in the curve from a to b and x to y (Rajeshkumar et al., 2021; Udhayakumar et al., 2023; Vijay et al.,

350 2021). At this stage, weight loss will be around 4% to 6% for the temperature rise from 25°C to 80°C.

351 When the temperature was raised to above 80°C, the fiber has very negligible weight loss which can

352 be considered as a straight line that is from point b to c and y to z, showing that fiber was thermally

353 stable between 80°C to 200°C. When compared to untreated fiber, alkaline-treated fiber has greater

354 thermal stability and can withstand temperatures up to 240°C. (Arun Ramnath et al., 2023; Binoj et

355 al., 2016; Jebadurai et al., 2019).

356 Next in 3rd region viz., from c to e and z to v heavy weight loss can be noticeable which was about

357 60% for the temperature rise of 200°C to 380°C. During this phase hemicellulose, α-cellulose, and

358 lignin gets decomposed. Most decomposition of cellulose occurs above 320°C (Ganapathy et al.,

359 2019; Rajeshkumar et al., 2021; Vinod et al., 2021). Alkaline-treated fiber consumes an additional

360 20°C to 30°C of temperature to decompose compared to UT fiber, this is because of the elimination

361 of non-cellulosic contaminates using alkaline treatment. This was also evidenced by DTG curve as

362 shown in figure 7. UT fiber takes 340°C of temperature to get weight loss, whereas treated fiber takes

363 up to 360°C of temperature, which proves that thermal performance was improved after alkaline

364 treatment (Ganapathy et al., 2019; Kathirselvam et al., 2019; Manimaran et al., 2018).

365 Final decomposition takes place at the temperature range of 380°C to 700°C, where the remaining

366 amorphous lignin and waxy substances get decomposed. The weight loss was found to be 14% and

367 11% for UT and AT fiber respectively. The elimination of an undesirable component from the fiber

368 during the alkaline treatment accounts for the variation in weight loss (Vijay et al., 2021; Vinod et

369 al., 2021). As a result, both TGA and DTG curves were very useful in finding the thermal stability

370 for both fibers.

Table 7. Consolidated TGA results of both fibers

| Curve points | | Temperature (ºC) | % of weight loss | Decomposition |
Untreated Fiber	Treated Fiber			
a to b	x to y	25 to 80	6% and 4%	Moisture removal
b to c	y to z	80 to 200 and 80 to 240	Negligible	Thermally stable
c to e	z to v	200 to 340 and 240 to 380	60%	Cellulose decompose
e to f	v to t	above 360	14% and 11%	Wax and amorphous lignin
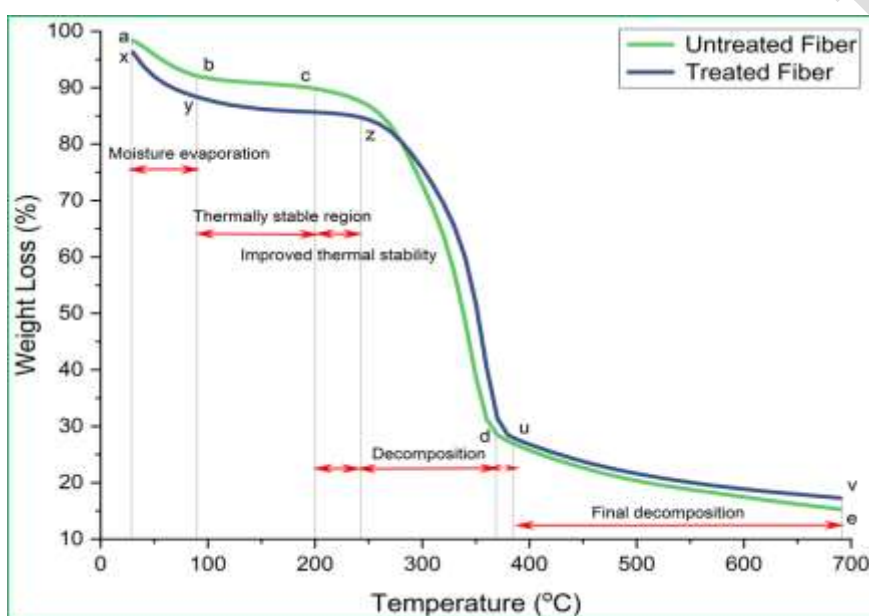
**Figure 7.** Thermogravimetric analysis of UT and AT of agave decipiens fiber
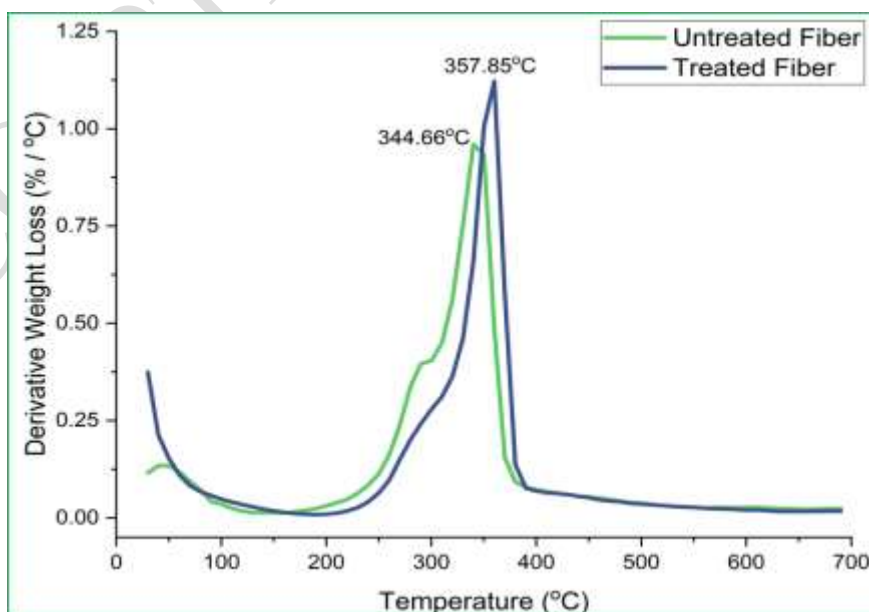
Figure 8. Derivative thermogravimetric of untreated and treated agave decipiens fiber

20

3.7. Differential Scanning Calorimetry

Figure 9 shows the DSC curvature for untreated and alkaline-treated agave decipiens fiber. DSC curve is used to support the TGA analysis for the same fiber. From figure 9 it can be noted that an endothermic peak occurs between 60°C to 80°C in both fibers. During this phase, the moisture absorbs the heat supplied to the fiber and gets evaporated (Madhu et al., 2019; Madhu et al., 2020; Narayanasamy et al., 2020). Temperature around 150°C to 170°C is known as glass transition phase. Fiber starts changing its phase to crystallinity where most of the hemicellulose and other unwanted substances get degraded. The curve moves upward at the temperature above 250°C, where the crystallinity peak occurs. At this phase, a small amount of amorphous lignin and cellulose were removed And above 350°C, the exothermic peak occurs during which all the constituents get burnt up (Ganapathy et al., 2019; Kathirselvam et al., 2019; Madhu et al., 2020; Zakikhani et al., 2014). The DSC curve well agrees with the TGA results for UT and AT fiber.
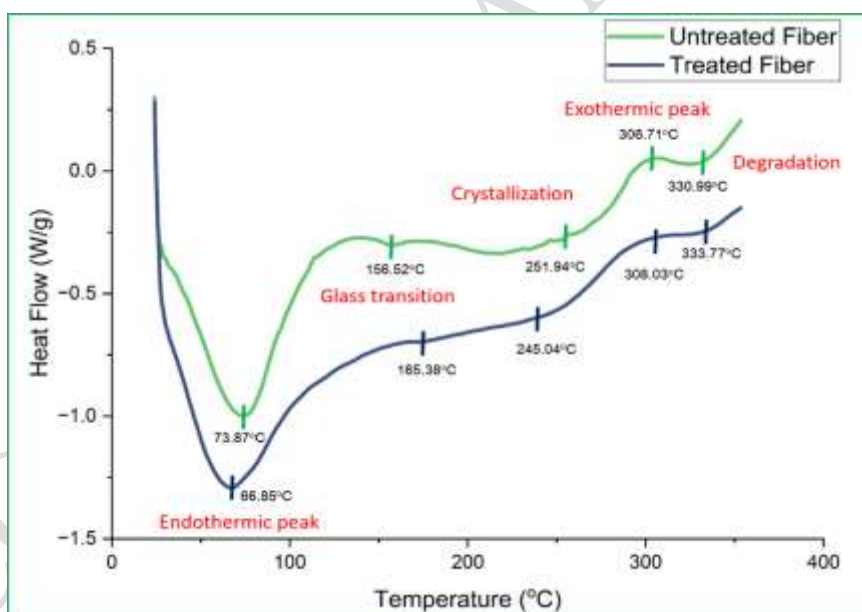
Figure 9. Differential Scanning Calorimetry for UT and AT fiber

*3.8. Scanning Electron Microscope*

SEM micrographs for both UT and AT of agave decipiens fiber were obtained from examination, which was shown in figures 10 and 11. SEM morphology is a good method to understand and study the outer structure of the fiber, mainly it is useful in investigating the change in the outer surface before and after surface modification.

21

395 In the UT fiber small micro-fibrils and other surface impurities can be clearly visualized in figure 10

396 (a) & (b). Absence of micro-fibrils and non-cellulosic impurities was prominently able to be seen in

397 the micrograph (i.e.) in figure 11 (a). Compared to UT fiber, AT fiber looks clean and roughness has

398 been developed on the fiber surface which was given in figure 11 (b).

399 Presence of roughness over the surface helps the fiber to properly merges with the resin during

400 reinforcement (Arun Ramnath et al., 2023; Manimaran et al., 2018; Manimaran et al., 2022;

401 Shanmugasundaram et al., 2018). From SEM micrographs it was able to understand that alkaline

402 treatment made some impact on the agave decipiens fiber.

403
404 **(a)** **(b)**

405 **Figure 10.** Fiber with impurities and micro-fibrils

406
407 **(a)** **(b)**
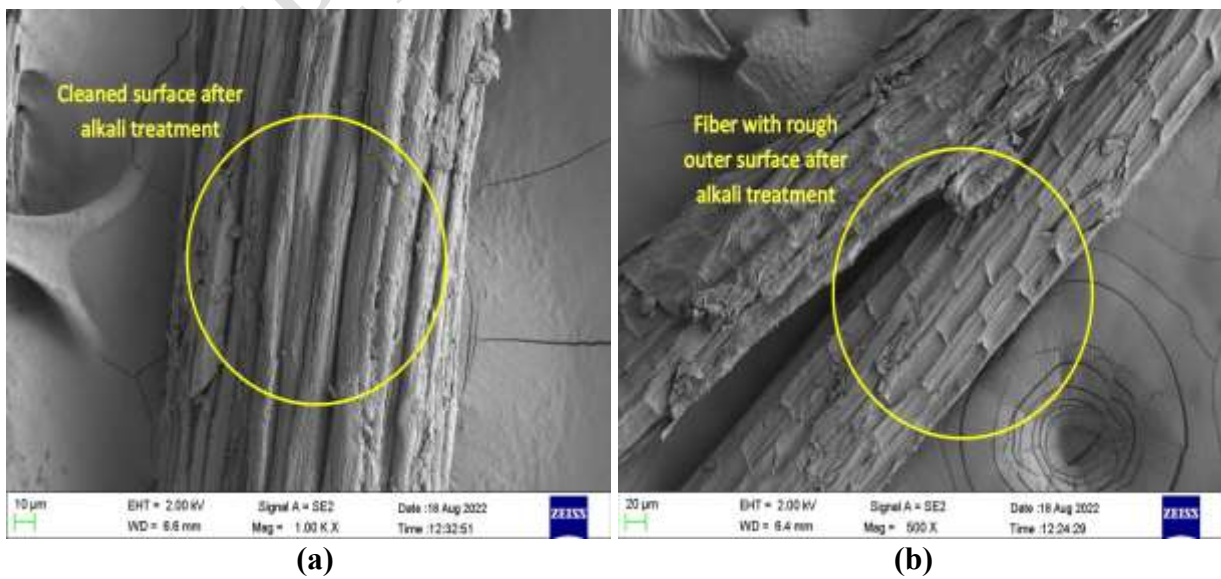
408 **Figure 11.** Fiber with a clean and rough surface

22

4. Conclusion

Agave decipiens a new plant fiber was successfully extracted by mechanical decortication method and imparted to chemical treatment using sodium hydroxide with 5% (w/v) concentration. In this research work characterization of both UT and AT of agave decipiens fiber was executed. Amount of chemical components present in both fibers was obtained using chemical composition analysis, in which the cellulose content gets improved due to the deduction of unwanted cellulosic components and impurities. This change in chemical composition was supported by FT-IR spectroscopy analysis. An increase in cellulose content directly increases the crystallinity in the fiber which was proved by the X-Ray diffractogram. Tensile test on single fiber confirms the increase of tensile modulus in alkaline-treated fiber. The thermal decomposition of UT and AT of agave decipiens fiber was studied using TGA, in which fiber treated with alkaline solution withstands higher temperature than untreated fiber. Using SEM micrographs the morphology of the fiber was studied. In untreated fiber, small micro-fibrils and impurities were able to be identified. Meanwhile, in alkaline treated fiber, the surface looks clean and roughness was created because of the impact produced by the NaOH reaction with fiber. This change was able to identify by outer diameter measurement from that reduction of diameter can be witnessed in alkaline treated fiber. From this research study, various properties of newly identified plant fiber (agave decipiens fiber) were successfully characterized for both untreated and alkaline-treated fiber. Experimental results proved that the agave decipiens fiber can be used as a reinforcement after performing chemical treatment. In a future study, the impact of varying concentrations of alkaline solution or different chemical treatments can be investigated and compared.

Conflict of Interest

Declaring no conflict of interest.

References

432   Arun Ramnath R., Murugan S., Sanjay M.R., Vinod A., Indran S., Elnaggar A.Y. and Siengchin S.

433   (2023), Characterization of novel natural cellulosic fibers from abutilon indicum for potential

434   reinforcement in polymer composites, *Polymer Composites*, **44(1)**, 340-355.

435   Babu B.G., Princewinston D., Saravanakumar S.S., Khan A., Aravind Bhaskar P.V., Indran S. and

436   Divya D. (2022), Investigation on the physicochemical and mechanical properties of novel alkali-

437   treated phaseolus vulgaris fibers, *Journal of Natural Fibers*, **19(2)**, 770-781.

438   Binoj J.S., Raj R.E., Sreenivasan V.S. and Thusnavis G.R. (2016), Morphological, physical,

439   mechanical, chemical and thermal characterization of sustainable Indian areca fruit husk fibers

440   (Areca catechu L. as potential alternate for hazardous synthetic fibers, *Journal of Bionic

441   Engineering,* **13(1)**, 156-165.

442   Chakravarthy S., Madhu S., Raju J.S.N. and Md J.S. (2020), Characterization of novel natural

443   cellulosic fiber extracted from the stem of cissus vitiginea plant, *International Journal of

444   Biological Macromolecules*, **161**, 1358-1370.

445   Ding L., Han X., Cao L., Chen Y., Ling Z., Han J. and Jiang S. (2022), Characterization of natural

446   fiber from manau rattan (calamus manan) as a potential reinforcement for polymer-based

447   composites, *Journal of Bioresources and Bioproducts*, **7(3)**, 190-200.

448   Ganapathy T., Sathiskumar R., Senthamaraikannan P., Saravanakumar S.S. and Khan A. (2019),

449   Characterization of raw and alkali treated new natural cellulosic fibres extracted from the aerial

450   roots of banyan tree, *International Journal of Biological Macromolecules,* **138**, 573-581.

451   Guo A., Sun Z. and Satyavolu J. (2019), Impact of chemical treatment on the physiochemical and

452   mechanical properties of kenaf fibers, *Industrial Crops and Products*, **141**, 111726.

453   Hamidon M.H., Sultan M.T., Ariffin A.H. and Shah A.U. (2019), Effects of fibre treatment on

454   mechanical properties of kenaf fibre reinforced composites: a review, *Journal of Materials

455   Research and Technology,* **8(3)**, 3327-3337.

456   Jaiswal D., Devnani G.L., Rajeshkumar G., Sanjay M.R. and Siengchin S. (2022), Review on

457   extraction, characterization, surface treatment and thermal degradation analysis of new cellulosic

458   fibers as sustainable reinforcement in polymer composites, *Current Research in Green and*

459   *Sustainable Chemistry*, **5**, 100271.

460   Jebadurai S.G., Raj R.E., Sreenivasan V.S. and Binoj J.S. (2019), Comprehensive characterization of

461   natural cellulosic fiber from cocciniagrandis stem, *Carbohydrate Polymers*, **207**, 675-683.

462   Kabir M.M., Wang H., Lau K.T. and Cardona F. (2012), Chemical treatments on plant-based natural

463   fibre reinforced polymer composites: an overview, *Composite B Engineering*, **43(7)**, 2883-2892.

464   Kathirselvam M., Kumaravel A., Arthanarieswaran V.P. and Saravanakumar S.S. (2019),

465   Characterization of cellulose fibers in thespesiapopulnea barks: influence of alkali treatment,

466   *Carbohydrate Polymers*, **217**, 178-189.

467   Khan A., Vijay R., Singaravelu D.L., Sanjay M.R., Siengchin S., Verpoort F. and Asiri A.M. (2021),

468   Extraction and characterization of natural fiber from eleusine indica grass as reinforcement of

469   sustainable fiber reinforced polymer composites, *Journal of Natural Fibers*, **18(11)**, 1742-1750.

470   Komal U.K., Verma V., Ashwani T., Verma N. and Singh I. (2018), Effect of chemical treatment on

471   thermal, mechanical and degradation behavior of banana fiber reinforced polymer composites,

472   *Journal of Natural Fibers*.

473   Krika F., Krika A. and Azizi A. (2021), Impact of NaOH-surface treatment on emerging pollutant

474   biosorption performance using marine algua, Posidonia Oceanica, *Global Nest Journal*, **23(1)**,

475   127-136.

476   Kumar K.P. and Sekaran A.S.J. (2014), Some natural fibers used in polymer composites and their

477   extraction processes: a review, *Journal of Reinforced Plastics and Composites*, **33(20)**, 1879-

478   1892.

479 Latif R., Wakeel S., Zaman Khan N., Noor Siddiquee A., Lal Verma S. and Akhtar Khan Z. (2019),

480 Surface treatments of plant fibers and their effects on mechanical properties of fiber-reinforced

481 composites: a review, *Journal of Reinforced Plastics and Composites*, **38(1)**, 15-30.

482 Liu Y., Lv X., Bao J., Xie J., Tang X., Che J. and Tong J. (2019), Characterization of silane treated

483 and untreated natural cellulosic fibre from corn stalk waste as potential reinforcement in polymer

484 composites, *Carbohydrate Polymers*, **218**, 179-187.

485 Maache M., Bezazi A., Amroune S., Scarpa F. and Dufresne A. (2017), Characterization of a novel

486 natural cellulosic fiber from juncus effusus L., *Carbohydrate Polymers*, **171**, 163-172.

487 Madhu P., Sanjay M.R., Jawaid M., Siengchin S., Khan A. and Pruncu C.I. (2020), A new study on

488 effect of various chemical treatments on agave americana fiber for composite reinforcement:

489 physico-chemical, thermal, mechanical and morphological properties, *Polymer Testing*, **85**,

490 106437.

491 Manimaran P., Senthamaraikannan P., Sanjay M.R., Marichelvam M.K. and Jawaid M. (2018), Study

492 on characterization of furcraea foetida new natural fiber as composite reinforcement for

493 lightweight applications, *Carbohydrate Polymers*, **181**, 650-658.

494 Manimaran P., Vignesh V., Khan A., Pillai G.P., Nagarajan K.J., Prithiviraj M. and Asiri A.M.

495 (2022), Extraction and characterization of natural lignocellulosic fibres from typhaangustata

496 grass, *International Journal of Biological Macromolecules*, **222**, 1840-1851.

497 Madhu P., Sanjay M.R., Pradeep S., Bhat K.S., Yogesha B. and Siengchin S. (2019), Characterization

498 of cellulosic fibre from phoenix pusilla leaves as potential reinforcement for polymeric

499 composites. *Journal of Materials Research and Technology*, **8(3)**, 2597-2604.

500 Moshi A.A.M., Ravindran D., Bharathi S.S., Indran S., Saravanakumar S.S. and Liu Y. (2020),

501 Characterization of a new cellulosic natural fiber extracted from the root of ficus religiosa tree.

502 *International Journal of Biological Macromolecules*, **142**, 212-221.

503 Narayanasamy P., Balasundar P., Senthil S., Sanjay M.R., Siengchin S., Khan A. and Asiri A.M.

504   (2020), Characterization of a novel natural cellulosic fiber from calotropis gigantea fruit bunch

505   for eco-friendly polymer composites, *International Journal of Biological Macromolecules*, **150**,

506   793-801.

507 Neto J.S.S., Lima R.A.A., Cavalcanti D.K.K., Souza J.P.B., Aguiar R.A.A. and Banea M.D. (2019),

508   Effect of chemical treatment on the thermal properties of hybrid natural fiber-reinforced

509   composites, *Journal of Applied Polymer Science*, **136(10)**, 47154.

510 Prithiviraj M. and Muralikannan R. (2022), Investigation of optimal alkali-treated perotis indica plant

511   fibers on physical, chemical, and morphological properties, *Journal of Natural Fibers*, **19(7)**,

512   2730-2743.

513 Puspita A.S., Budihardjo M.A. and Samadikun B.P. (2023), Evaluating coconut fiber and fly ash

514   composites for use in landfill retention layers, *Global Nest Journal*, **25(4)**, 1-7.

515 Rajeshkumar G., Devnani G.L., Maran J.P., Sanjay M.R., Siengchin S., Al-Dhabi N.A. and

516   Ponmurugan K. (2021), Characterization of novel natural cellulosic fibers from purple bauhinia

517   for potential reinforcement in polymer composites, *Cellulose*, **28(9)**, 5373-5385.

518 Ramakrishnan T., Senthil Kumar S., Samuel Chelladurai S.J., Gnanasekaran S., Geetha N.K.,

519   Arthanari R. and Debtera B. (2022), Effect of moisture content on mechanical properties of AAM

520   natural fiber-reinforced isophthalic polyester composites, *Advances in Materials Science and*

521   *Engineering*, 1-10.

522 Ramshankar P., Sashikkumar M., Ganeshan P. and Raja K. (2023), Experimental investigation of

523   hybrid composites using biowastes and Calotropis gigantea: an eco-friendly approach, *Global*

524   *Nest Journal*, **25(4)**, 70-76.

525 Ravindran D., Sundara Bharathi S.R., Padma S.R., Indran S. and Divya D. (2020), Characterization

526   of natural cellulosic fiber extracted from grewia damine flowering plant's stem, *International*

527   *Journal of Biological Macromolecules*, **164**, 1246-1255.

528   Reddy K.O., Ashok B., Reddy K.R.N., Feng Y.E., Zhang J. and Rajulu A.V. (2014), Extraction and

529   characterization of novel lignocellulosic fibers from thespesia lampas plant, *International*

530   *Journal of Polymer Analysis and Characterization*, **19(1)**, 48-61.

531   Santos J.C.D., Oliveira P.R., Freire R.T.S., Vieira L.M.G., Rubio J.C.C. and Panzera T.H. (2022),

532   The effects of sodium carbonate and bicarbonate treatments on sisal fibre composites, *Materials*

533   *Research*, **25**.

534   Sarala R. (2020), Characterization of a new natural cellulosic fiber extracted from derris scandens

535   stem, *International Journal of Biological Macromolecules*, **165**, 2303-2313.

536   Sgriccia N., Hawley M.C. and Misra M. (2008), Characterization of natural fiber surfaces and natural

537   fiber composites. *Composites - A: Applied Science and Manufacturing*, **39(10)**, 1632-1637.

538   Shaker K., Khan R.M., Jabbar M., Umair M., Tariq A., Kashif M. and Nawab Y. (2020), Extraction

539   and characterization of novel fibers from vernonia elaeagnifolia as a potential textile fiber,

540   *Industrial Crops Products*, **152**, 112518.

541   Shanmugasundaram N., Rajendran I. and Ramkumar T. (2018), Characterization of untreated and

542   alkali treated new cellulosic fiber from an areca palm leaf stalk as potential reinforcement in

543   polymer composites, *Carbohydrate Polymers*, **195**, 566-575.

544   Thirumalaisamy R. and Subramani S.P. (2018), Investigation of physico-mechanical and moisture

545   absorption characteristics of raw and alkali treated new agave angustifolia marginata (AAM)

546   fiber, *Materials Science*, **24(1)**, 53-58.

547   Udhayakumar A., Mayandi K., Rajini N., Devi R.K., Muthukannan M. and Murali M. (2023),

548   Extraction and characterization of novel natural fiber from cryptostegia grandiflora as a potential

549   reinforcement in biocomposites, *Journal of Natural Fibers*, **20(1)**, 2159607.

550   Venkatachalam N., Navaneethakrishnan P., Rajsekar R. and Shankar S. (2016), Effect of pretreatment

551   methods on properties of natural fiber composites: a review, *Polymers and Polymer Composites*,

552   **24(7)**, 555-566.

553   Vinod A., Vijay R., Singaravelu D.L., Sanjay M.R., Siengchin S., Yagnaraj Y. and Khan S. (2021),

554   Extraction and characterization of natural fiber from stem of cardio spermum halicababum,

555   *Journal of Natural Fibers*, **18(6)**, 898-908.

556   Vijay R., Singaravelu D.L., Vinod A., Paul Raj I.F., Sanjay M.R. and Siengchin S. (2020),

557   Characterization of novel natural fiber from saccharum bengalense grass (Sarkanda), *Journal of*

558   *Natural Fibers*, **17(12)**, 1739-1747.

559   Vijay R., Manoharan S., Arjun S., Vinod A. and Singaravelu D.L. (2021), Characterization of silane-

560   treated and untreated natural fibers from stem of leucasaspera, *Journal of Natural Fibers*, **18(12)**,

561   1957-1973.

562   Vijay R., James Dhilip J.D., Gowtham S., Harikrishnan S.B.M.A., Chandru B., Amarnath M. and

563   Khan A. (2022), Characterization of natural cellulose fiber from the barks of vachellia farnesiana,

564   *Journal of Natural Fibers*, **19(4)**, 1343-1352.

565   Zakikhani P., Zahari R., Sultan M.T.H. and Majid D.L. (2014), Extraction and preparation of bamboo

566   fibre-reinforced composites, *Materials & Design*, **63**, 820-828.